Proc Indian Natn Sci Acad, **70, A,** No. 3, May 2004, pp. 503-514

ELECTROREDUCTION OF MONOMERIC MOLYBDATE(VI) ON GLASSY CARBON ELECTRODE IN H_2SO_4 SOLUTIONS I. ADSORPTION AND COUPLED CATALYTIC REACTIONS IN Mo(VI) REDUCTION IN 0.1 M H_2SO_4

K CHANDRASEKARA PILLAI*, G ILANGOVAN AND S M SENTHIL KUMAR

Department of Physical Chemistry, University of Madras, Guindy Campus, Chennai-600 025 (India)

(Received 12 November 2002; Accepted 22 April 2003)

A study of the cathodic reduction of molybdate(VI) on a glassy carbon electrode in 0.1 M H_2SO_4 has been carried out over a wide range of experimental conditions. Electrochemical (cyclic voltammetry, constant potential electrolysis) and spectroscopic (UV and X-ray photoelectron) techniques for product analysis have been used. Molybdate(VI) exhibits five reduction peaks (C1, C2, C3, C4, and C5). Controlled potential bulk electrolysis gives number of electrons (net) exchanged per molecule of Mo(VI) as one, indicating that all the five reduction peaks to be due to the Mo(VI) to Mo(V). The first two peaks C1 and C2 are due to reversible reduction of two forms of molybdate(VI) species adsorbed on the surface. These peaks analysed using the surface activity theory for immobilised molecules at the electrode as described by Brown and Anson (*Anal Chem* **49** (1977) 1589) show repulsive interaction for C1 and attractive interaction for C2 at saturation surface condition. These processes involve two independent one-electron transfer steps at C1 and C2 that yield molybdate(V) species, also immobilised at the electrode, which undergoes a further reduction at C3 to an adsorbed component molybdate(III). In addition, the Mo(VI) reactant ions that reach the surface by diffusion and the surface bound product molybdate(III) react to generate the molybdate(V)$_{ads}$. The rate constant of the catalytic regeneration step calculated from the CV data is $(0.60 \pm 0.15) \times 10^3$ $M^{-1}s^{-1}$. The C4 and C5 peaks are due to two independent one-electron transfer quasireversible reduction of two forms of Mo(VI) species diffusing to the electrode. The reduction at C4 and C5 show additionally the features of weak reactant adsorption.

Key Words: Electroreduction; Monomeric Molybdate (VI); Glassy Carbon Electrode; Cyclic Voltammetry; Adsorption; Coupled Catalytic Reaction; Solution Equilibrium; UV; XPS

Introduction

Electroreduction of monomeric molybdate(VI) in both complexing and noncomplexing acids remains as a subject of continuing interest for two main reasons: the electroreduced product has been known to yield catalytic currents in presence of certain anions in solution (NO_3^-, ClO_4^-, ClO_3^- etc), which has been utilised as a method of estimating Mo(VI)/anion[1] ; the Mo(VI) reduction exhibits highly complex behaviour depending on the nature of the acid and the concentrations of the acid and Mo(VI) ions in solution[2-11]. In solutions of moderate to high acid concentrations (0.01 M and above), in which molybdate(VI) is present as monomeric and dimeric species[6,12-15], two, three, four reduction waves have been reported by various authors in polarographic studies and related techniques[2-11]. But in all cases the Mo(VI) reduction products in solution have been identified to be pentavalent and trivalent forms. Several hypotheses have been proposed to explain the origin of these multiple peaks. While successive electron transfer steps through various oxidation states +5, +4, and +3 have been suggested by some authors[11] as prime cause, reduction of different species of Mo(VI), which are in slow equilibrium in acid solutions, has been considered as responsible by others[3,5]. Ideas such as existence of the reduction products Mo(V) and /or Mo(III) in several different forms in solution have also been postulated[7]. Apart from little information about the reactants involved in each polarographic wave, there are several conflicting interpretations on the mechanism of Mo(VI) ion reduction on Hg electrode.

Inspite of extensive work regarding electroreduction of monomeric molybdae(VI) on Hg electrode[1-11], its reduction on solid electrodes seems to have evoked limited interest[16-24]. Here the studies have chiefly been concerned with indirectly estimating Mo(VI) by making use of Pt[16] and graphite[17] electrodes.

*Author for Correspondence *E-mail:* kc_pillai@yahoo.com
Fax : +91-44-2352870

Only few investigations dealing with reduction mechanisms have been reported[18,19]. Zanello *et al.* [18] have found that in 0.8-1.6 M H_2SO_4, Mo(VI) reduction occurs in two consecutive steps corresponding to Mo(VI) to Mo(V) and Mo(V) to Mo(III) on hydrogenated Pt, whereas only one reduction peak seems to occur on Pt (and Ni) in acetic acid solutions of pH 2 to 10[19]. In a previous paper[20], we have shown that on a glassy carbon electrode (GCE) Mo(VI) reduction gives multiple peaks in 0.1 M H_2SO_4 similar to those exhibited at Hg electrode[2-11]; however, the reaction mechanisms have not been analysed in detail. In the present work, an extensive cyclic voltammetric (CV) investigation on Mo(VI) ion in 0.1 M H_2SO_4 is reported on a GCE with extended Mo(VI) concentrations, and the CV data are analysed in order to elucidate the Mo(VI) reduction mechanism and the accompanying phenomena.

Controlled potential electrolysis (CPE), UV and X-ray photoelecton spectroscopic (XPS) techniques are used to estimate the equivalent electron number and reaction products in cyclic voltammetric electrolysis.

Experimental Details

$(NH_4)_6Mo_7O_{24}.4H_2O$ was of analytical grade reagent obtained from BDH and used as received. Mo(VI) concentration in bulk solution was determined gravimetrically by precipitation of $PbMoO_4$[20]. Twice distilled water, further purified by passing it through charcoal column, was used for making up all the experimental solutions. Purified nitrogen was used to purge the solutions. Experiments were carried out in a three compartment cell. A platinum foil and SCE with luggin capillary were used as counter and reference electrodes. All potentials are referred with respect to SCE.

The CV unit contained Wenking Potentiostat (ST 72) coupled with Wenking scan generater (VSG 8) and Graphtec X-Y recorder (WX2300). Hewlett Packard UV-VIS diode array spectrometer (HP8452) was used for product analysis in constant potential experimemts. XPS measurements were carried out with VG Scientific ESCALAB MK II spectrometer.

The GCE of geometric area 0.07 cm^2 was hand polished with increasingly finer grades of emery papers (2/0, 3/0, 4/0 Winning Emery India) to mirror finish, degreased with trichloroethylene, washed with copious amount of double distilled water. The polished electrode was cycled in deaerated 0.1 M H_2SO_4 for 20 times between the potentials +0.70 V to –1.0 V at a scan rate of 20 mV s^{-1}, washed and introduced into the deaerated experimental solutions. Before each CV measurement, GC electrode was pretreated following the above procedure. All the experiments were carried out at 25± 0.2°C.

For curve fitting analysis of the cyclic voltammograms, the current potential data of 10 mV intervals were used. Computations were carried out in FORTRAN 77 using an IBM compatible microcomputer.

Results and Discussion

Typical cyclic voltammograms of 2 mM Mo(VI) in 0.1 M H_2SO_4 under different potential windows are illustrated in Fig.1. In the potential range +500 mV to –1000 mV five reduction peaks C1, C2, C3, C4 and C5 appear at peak potentials +240, +130, -120, -350 and –450 mV. One broad oxidation peak A4, accompanying with a shoulder A5 at a more negative potential, appears at –270 mV in the reverse sweep (Fig.1, Curve(a)). When the sweep range is limited to –200 mV, the three anodic peaks A1, A2 and A3 appear (Fig.1, curve(b)). The number for each peak is given in such a way that the same number for the cathodic and anodic peak makes a redox couple. The anodic counter parts of the cathodic peaks are identified by varying the switching potential in CV.

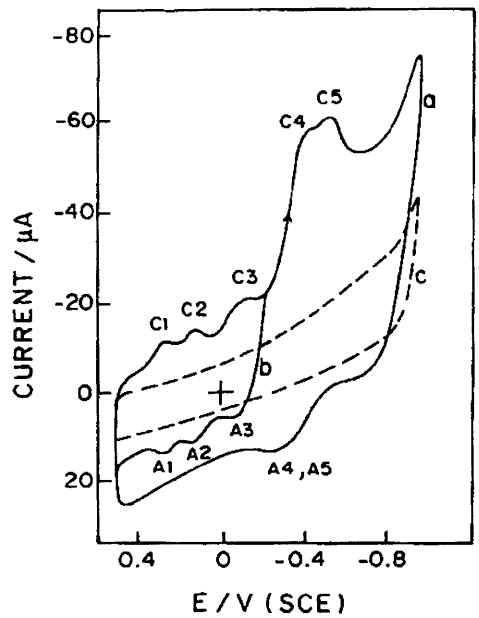

Fig. 1 Cyclic voltammograms of 2 mM Mo(VI) in 0.1 M H_2SO_4 recorded in different potential range: (a) between +0.5 and –1.0 V (SCE); (b) between +0.5 and –0.2 V(SCE); (c) (----) CV of bare GCE in 0.1 M H_2SO_4 alone (scan rate = 400 mVs^{-1})

At different scan rates ranging from 5 to 600 mV s^{-1} and over a concentration range of 0.3 to 12 mM of Mo(VI) in solution, voltammograms qualitatively similar to those presented in Fig.1 are observed except for the anodic peaks A3, A4 and A5. The detailed analyses are given below for individual redox pairs.

Processes at C1/A1 and C2/A2

Fig. 2A shows CV of 2 mM Mo(VI) at various scan rates recorded up to –100 mV encompassing C1/A1 and C2/A2. The cyclic voltammetric data are summarised in Table I for C1/A1. The cyclic voltammetric behaviour and the CV data for C1/A1 are the same, even when the voltammograms are recorded covering only C1/A1. The peaks C2/A2 also display similar data, signifying that the redox couples C1/A1 and C2/A2 represent two independent processes. The features of the two pairs of redox peaks are the following: (i) $\log(i_{pc})$ vs $\log(\nu)$ plots show a slope of unity; (ii) anodic peak current (i_{pa}) to cathodic peak current (i_{pc}) ratio is unity irrespective of ν; (iii) current

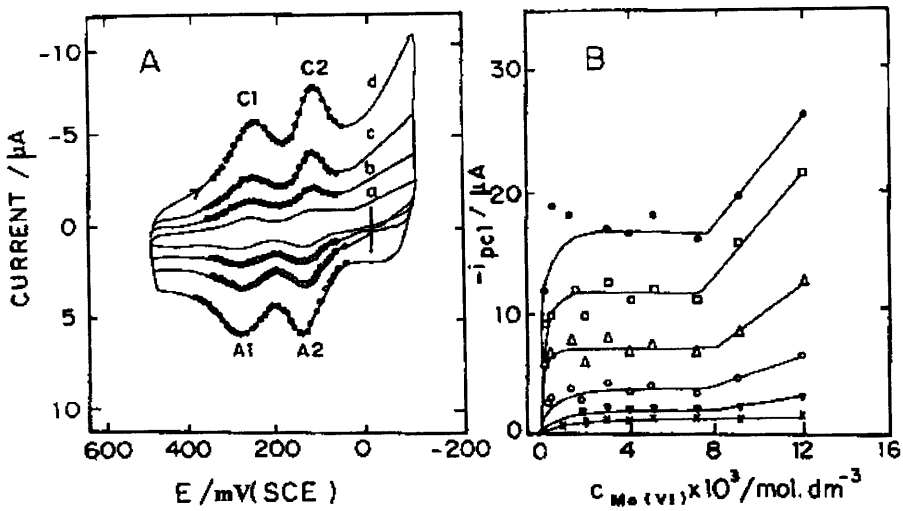

Fig. 2 (A) Cyclic voltammograms (C1/A1 and C2/A2 peaks) of 2 mM Mo(VI) in 0.1 M H_2SO_4 at different scan rates (mVs^{-1}): (a) 20; (b) 50; (c) 100; (d) 200. Solid lines are experimental curves. (**O**) Points calculated from nonlinear regression onto eqns. (2) to (4) (see the text). (B) Dependence of peak current on $c_{Mo(VI)}$ in 0.1 M H_2SO_4 for C1 peak at different scan rates (mVs^{-1}) : (**X**) 20; (▼)50; (**o**) 100; (Δ) 200; (□) 400; (●) 600.

Table I

Cyclic Voltammetric Characteristics of C1/A1 Peaks in 0.1 M H_2SO_4

$C_{Mo(VI)}$/mM	v / mVs^{-1}	E_{pc1}/mV(SCE)	ΔE_p (E_{pA1}- E_{pc1})/mV	E_{FWHM}/mV	i_{pA1}/ $\lvert i_{pc1}\rvert$	10^{-4} $_{(ipc1/C_{MO(vi)v})}$[a]
0.5	20	235	20	70.0	1.00	5.00
	50	228	22	70.0	1.0	5.20
	100	225	25	75.0	1.02	5.60
	150	228	15	85.0	0.98	6.60
	200	225	18	90.0	1.04	6.25
	300	225	18	95.0	1.03	5.33
	400	225	15	110.0	1.12	4.25
	600	225	10	135.0	1.04	4.00
1.5	100	270	18	75.0	1.10	2.58
2.0	100	270	20	90.0	1.00	1.33
3.0	100	285	20	90.0	1.00	1.33
4.0	100	290	20	90.0	1.27	0.81
5.0	100	290	20	102.5	1.17	0.70
7.0	100	275	30	95.0	1.20	0.40
9.0	100	268	33	120.0	0.94	0.50
12.0	100	273	28	107.5	0.82	0.52

[a] μ A dm^3 s v^{-1} mol^{-1}

function ($i_{pc}/c_{Mo(VI)}\nu$) remains constant at all ν studied; and (iv) a slight shift in the peak potential of C1 (E_{pC1}) of -9.9 ± 4.4 mV/log(ν) is observed. These are strong evidences for adsorption of a species that undergoes a reversible electrochemical reaction in the adsorbed state. However, the anodic and cathodic peak separation (ΔE_p) is around 20 mV for both redox couples (Table I), different from zero predicted for a reversible surface redox process[25]. Also, full width at half maxima (E_{FWHM}) of the cathodic and anodic peaks are around 70 mV at ν =20 mVs^{-1} (Table I), compared to the theoretical value of 90.6/n mV[25,26], where n is the number of electrons transferred per electroactive species. These deviations could be caused by non-ideal behaviour of adsorbed moieties due to interactions in the adsorbed layer[25,26]. For a reversible non-ideal adsorption peak, the electron transfer number n can be obtained following the method suggested by Facci and Murray[27], from the experimentally measured E_{FWHM} values, the working plot given in ref. [26], and the relation for the peak current. n values computed by this method are 1.3±0.1 and 1.3±0.1 for C1 and C2 respectively. These results suggest that one electron is involved in the redox couple for the adsorbates at C1 and C2.

Fig. 2B shows that there is a tendency for i_{pC1} to increase linearly with $c_{Mo(VI)}$ at very low concentrations below 0.5 mM, and above 1 mM a limiting value is reached due to complete surface coverage. After surface saturation i_{pC1} increases further with Mo(VI) concentration beyond 7 mM. This unusual increase in peak current with increasing $c_{Mo(VI)}$ must be related to a new faradaic process. Taking into account that even at these higher concentrations the current function $i_{pC1}/c_{Mo(VI)}\nu$ decreases with $c_{Mo(VI)}$ (Table I), which is characteristic of adsorption controlled process, the excess current may involve the adsorbate acting as a electron carrier between the electrode and Mo(VI) in solution[28].

XPS analyses of GCE surface are performed after polarising the electrode at 150 mV (after C1) or 60 mV (after C2) for 2 hours in 0.1 M H_2SO_4 containing 2 mM Mo(VI). The high resolution spectra of Mo 3d level is shown in Fig.3, which also includes Mo 3d spectra of standard substance $(NH_4)_6Mo_7O_{24}.4\ H_2O$. The standard substance gives rise to two deconvoluted peaks (Fig. 3(A)) at binding energies (BE) 233.4 and 236.5 eV corresponding to $3d_{5/2}$ and $3d_{3/2}$ levels with intensity ratio 3:2.4, consistent with Mo in the oxidation state +6[29]. The electrodes polarised after C1 or C2 give BE values corresponding to Mo(V)[30] on the electrode surface (Table II). Thus the product formed is the one-electron reduction product, viz., Mo(V), at C1 as well as at C2.

Integration of the voltammetric peaks C1 and C2 provides the electrical charge Q_t exchanged in the overall reduction process at each of the peaks. From the charge, the maximum surface concentration $\tau^0_{Mo(VI)}$ is calculated.

$$Q_t = \int_0^t i\,dt = nFA_{geo}\,\tau^0_{Mo(VI)}\,\theta_{Mo(VI)} = Q_m\,\theta_{Mo(VI)} \quad \ldots (1)$$

where Q_m is the charge associated with the Mo(VI) monolayer ($=nFA_{geo}\,\tau^0_{Mo(VI)}$), A_{geo} is the geometric area of the electrode, $\theta_{Mo(VI)} = \tau_{Mo(VI)}/\tau^0_{Mo(VI)}$ and $\tau_{Mo(VI)}$ is the surface concentration of Mo(VI). The value obtained, Q_m = 3.54 μC, for C1 corresponds to 5.24×10^{-10} moles cm^{-2}, which is equivalent to an area of 31.7 $(A°)^2$ per molecule. For C2 peak the value is found to be 29.3 $(A°)^2$ per molecule. Such values indicate that adsorbates of quite a large size are present in the C1 and C2 regions[31].

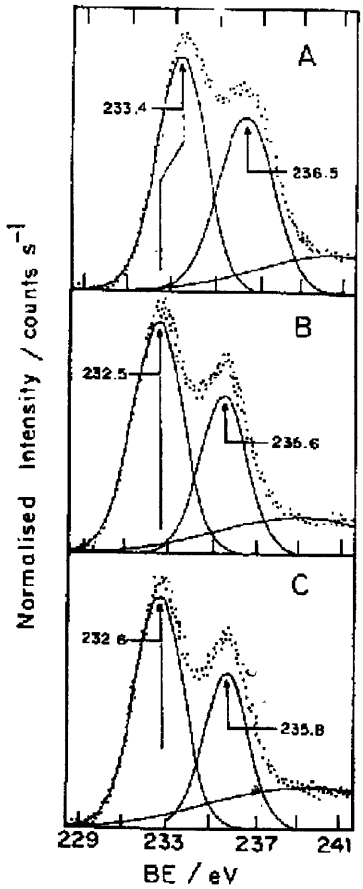

Fig. 3 Deconvoluted XPS spectra of Mo 3d level: (A) $(NH_4)_6Mo_7O_{24}.4H_2O$; (B) GCE polarised after peak C1; (C) GCE polarised after peak C2.

Table II

Binding Energy Values of Mo 3d level. (FWHM Values are given in parenthesis)

Sample	BE/eV		ΔBE/eV ($3d_{5/2}$ - $3d_{3/2}$)	Intensity ratio ($3d_{5/2}$: $3d_{3/2}$)	Mo Oxidation state
	$3d_{5/2}$	$3d_{3/2}$			
$(NH_4)_6.Mo_7O_{24}.4H_2O$	233.4 (3.2)	236.5 (3.7)	3.1	3 : 2.4	Mo(VI)
GCE polarised after peak C1	232.5 (3.2)	235.6 (3.1)	3.1	3 : 2	Mo(V)
GCE polarised after C2	232.6 (3.1)	235.8 (3.1)	3.2	3 : 2	Mo(V)

The type of interaction in the adsorption layer at C1 and C2 can be assessed by calculating the interaction term ($G\theta_t$) of the adsorbates. This is made on the basis of the following current potential expression developed for the reversible non-ideal reduction of immobilised molecules at the electrode[25,26,32].

$$-i|i|_{ads} = -\left[\frac{n^2F^2A_{geo}\nu\tau_t}{RT}\right]\left\{\frac{\exp(p)}{[(1+\exp(p))-G\theta_t\exp(p)]}\right\} \quad ...(2)$$

$$\text{where } p = \left(\frac{nF}{RT}\right)(E-E_{rp}) - ((0.5-f_O)G\theta_O) \quad ...(3)$$

$$\left(\frac{nF}{RT}\right)(E-E_{rp}) = (0.5-f_O)\,G\theta_t + \ln\left[\frac{fo}{(1-fo)}\right] \quad ...(4)$$

where E_{rp} is the reversible peak potential for the attached O_{ads}/R_{ads} couple, τ_t is the total concentration of material adsorbed on the electrode, $\tau_t = \tau_O + \tau_R$. f_O is the fraction of adsorbed molecules in the oxidised form given by $f_O = \tau_O/\tau_t$, $\theta_t = \tau_t / \tau_t^0$, τ_t^0 being the maximum τ_t. G is defined as $G = (a_{OO} - a_{RO}) + (a_{RR} - a_{OR})$, where a_{ij} terms represent Frumkin's parameters describing the interaction amongst the species i,j = O or R. All other symbols have their usual significance.

The back-ground corrected voltammetric data from peaks C1, A1, C2 and A2 are used to fit the eq. (2), and the unknown parameters E_{rp}, $G\theta_t$ and τ_t are evaluated. We have carried out their numerical fitting by using a nonlinear multidimensional regression method based on the Lavengberg-Marquardt algorithm[33]. f_O at each experimental value of potential, needed for regressing eq. (2), is evaluated within the program by solving eq. (4) by a Newton-Raphson subroutine[33] using E_{rp} and $G\theta_t$ as regression parameters. As can be seen in Fig.2A, the simulated voltammetric peaks are consistent with the experimental values.

Using the estimated parameters (E_{rp}, $G\theta_t$ and τ_t), the quantities E_p, i_p and E_{FWHM} are calculated with the help of the following equations[25,26,32]

$$E_p = E_{rp} \quad ...(5)$$

$$i_p = \left[\frac{n^2F^2A_{geo}\nu\tau_1}{RT}\right]\left\{\frac{1}{[4-G\theta_t]}\right\} \quad ...(6)$$

$$E_{FWHM} = \left[\frac{2RT}{nF}\right]\left[\text{InQ} - G\theta_t\left\{\frac{(Q-1)}{(2Q+2)}\right\}\right] \quad ...(7)$$

$$\text{where } Q = \frac{\left[6-G\theta_t + \left((G\theta_t-6)^2-4\right)^{1/2}\right]}{2} \quad ...(8)$$

to compare them with the experimentally measured values with assumed background correction. The E_p, i_p and E_{FWHM} quantities obtained by nonlinear regression analyses on data from C1 at various ν for 2 mM Mo(VI) (corresponding to θ_t=1), and those obtained for different θ_t at ν = 100 mVs^{-1} are presented in Table III. Calculated E_p and i_p differ with their measured values only marginally: E_p to an extent of 5.4% maximum and i_p around 6.7% (at ν = 100 $mV\ s^{-1}$). The average relative standard deviation (RSD) of the regression is 3.3% of the measured i_p indicating the goodness of fit. $G\theta_t$ is positive at low surface coverages and it becomes negative when θ_t approaches saturation value. But in the case of C2, $G\theta_t$ is positive at all θ_t including when θ_t = 1 (not shown). Interactions in the adsorption layer are thus seen to be different (at θ_t = 1) for the two peaks C1 (repulsion) and C2 (attraction), indicating that the reactants of C1 peak might be charged components, while neutral species might be the reactants of C2 peak.

Processes at C3/A3

Representative cyclic voltammograms recorded up to –200 mV (SCE) at different scan rates for 2mM are given in Fig. 4. The appearance of A3 depends on the scan rate. It is observed when sweep rates higher than 300 mVs^{-1} are used. The i_{pA3}/i_{ipC3} ratio tends to a value close to 1 as sweep rates are increased. The C3/A3 voltammograms exhibit a shape and sweep dependence characteristic of an electrochemical process in which a reversible charge transfer step is

Table III

Results of Non-linear Regression Analyses of Cathodic Peak of C1/A1 for Various $c_{Mo(VI)}$ in 0.1 M H_2SO_4

$C_{Mo(VI)}$ /mM	v/ mVs^{-1}	E_{pc}/mV(SCE)		$\|i_{pc}\|$ / μA		E_{FWHM}/mV		Γ_t X 10^{10} /	$G\theta_t$	RSD[a]%
		Meas	Calcul	Meas	Calcul	Meas	Calcul	(mol. cm^{-2})		
0.3	100	232	230	2.65	2.82	75.0	81.7	3.95	0.36	3.9
0.5	100	225	226	2.85	2.99	75.0	80.1	5.91	0.41	4.1
1.0	100	230	232	2.00	2.00	75.0	77.0	2.77	0.53	4.5
1.5	100	235	240	3.87	4.14	75.0	81.1	2.76	0.38	2.6
2.0	50	250	252	1.37	1.00	90.0	86.5	2.93	0.17	2.1
	100	240	248	2.00	1.86	90.0	95.0	3.12	-0.15	1.8
	150	235	244	3.50	3.41	115.0	92.9	3.54	-0.06	6.7
	200	230	239	550	4.69	110.0	94.6	3.70	-0.13	2.5
	400	233	239	9.75	8.49	130.0	95.4	3.42	-0.16	3.0
5.0	100	235	235	3.62	4.01	102.5	101.4	6.38	-0.35	2.2

[a]Relative standard deviation of the regression calculated as percent of peak current

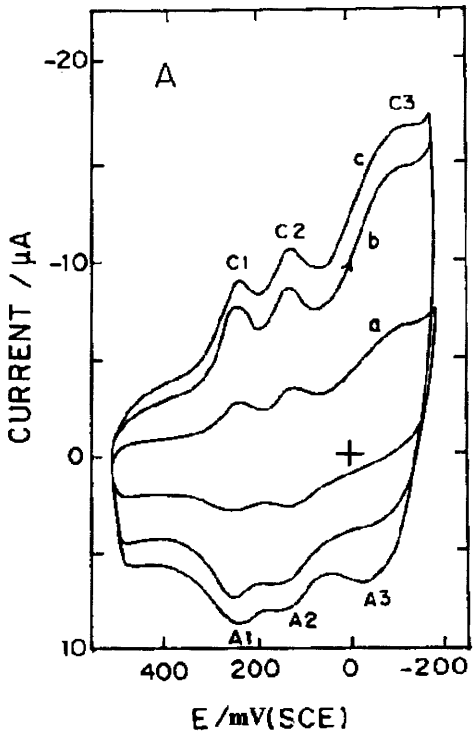

Fig. 4 Effect of scan rate on the voltammetric behaviour of C3/A3 peaks for 2 mM Mo(VI) in 0.1 M H_2SO_4 : (a) 200; (b) 300; (c) 400 mVs^{-1}

followed by a fast irreversible chemical reaction step. In an attempt to explore the follow-up process, we have carried out the following experiments.

Studies with Mo(VI) Modified GC Electrode (MGCE)

It is noted during these studies that the bare GC electrode, potential cycled between +500 to –300 mV (SCE) in Mo(VI) solution of any concentration, is taken out washed thoroughly with 0.1 M H_2SO_4 and introduced into the supporting electrolyte alone, it reproduces features analogues to bare GCE in Mo(VI) containing acid solution; except for the appearance of A3 peak. Curve (a) of Fig. 5 describes voltammogram recorded with a bare GCE in 2 mM Mo(VI) solution at 100 mVs^{-1}, where no A3 is present. However, the Mo(VI) modified GCE (MGCE) produces peak A3 (in addition to the other usual peaks C1, C2, C3, A1 and A2) in 0.1 M H_2SO_4 free of Mo(VI) (Fig. 5, curve (b)). The important feature that is noticed with MGCE is that it always gives A3 at all scan rates, including those which failed to give A3 at bare GCE in Mo(VI) containing solutions.

The results of Fig. 5 show that the process at C3/A3 is also a reversible electron transfer of an adsorbed redox couple as in the case of C1 and C2. The absence of A3 when Mo(VI) is available in solution can arise by the removal of the reduction product of C3 from the surface by Mo(VI) species present in solution through a fast irreversible chemical reaction step. By constant potential electrolysis (CPE) experiments, we have observed that the chemical reaction at C3 is a catalytic process. CPE was carried out, using a massive GCE plate of dimensions (8cm x 3cm x 0.3cm) on a solution of 0.5 mM Mo(VI) in 0.1M H_2SO_4, at –150 mV (i.e., after C3 peak). i-t curve recorded during CPE, and adsorption spectra recorded after CPE are shown in Fig. 6A and Fig. 6B respectively. The recorded current shows an initial increase followed by a slight decrease to a constant value which is maintained even after 5 hrs. Constancy of current at longer times is typical of processes involving catalytic regeneration of reactants[34]. The UV spectra of electrolysed solution after C3 shows absorption maxima at 254 and 294 nm which are characteristic of $Mo(V)_2$[5,8a]. Basing on these informations the processes at C3 of Fig.4 can be visualised as consisting of electrode-surface anchored

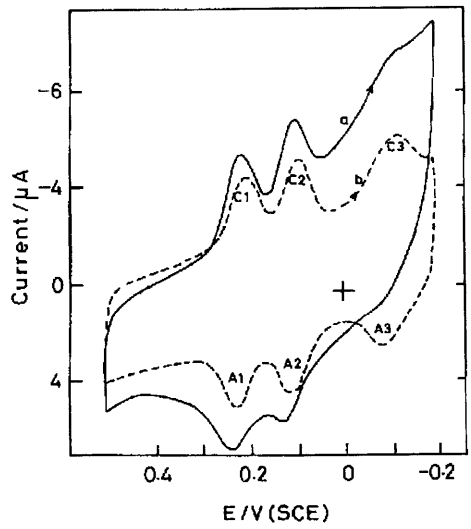

Fig. 5 Curve (a): Cyclic voltammogram of a bare GCE in 0.1 M H_2SO_4 solution containing 2 mM Mo(VI). Curve (b): Electrochemical response of Mo(VI) modified GCE (MGCE) in 0.1 M H_2SO_4 (MGCE was prepared by cycling the potential 10 times under the conditions as in curve (a)). (scan rate = 100 mVs^{-1})

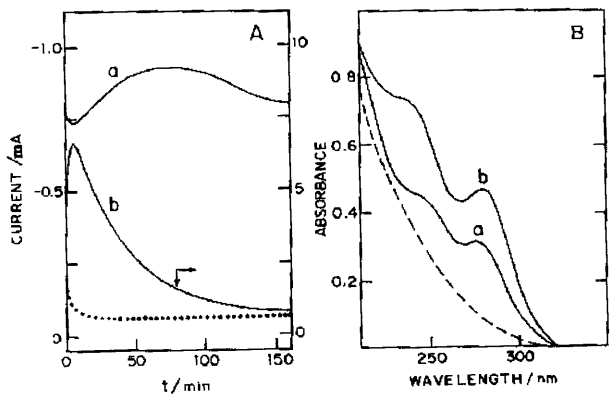

Fig. 6 Constant potential electrolysis of 0.5 M Mo(VI) in 0.1 M H_2SO_4 : (a) at –150 mV (after C3 peak); (b) at –500mV (after C5 peak). (A) i-t curves (dotted line represents i-t profile of bare GCE electrolysed at -500 mV in pure base electrolyte) (B) UV spectra of electrolysed solutions (broken line is the spectrum before electrolysis)

precatalyst (P_{ads}) / catalyst (Q_{ads}) sites catalysing the reduction of the substrate present in solution ($Mo(VI)_{sol}$)[35]; and can be represented as

$$P_{ads} + 2e \rightleftarrows Q_{ads} \quad \text{(catalyst couple } (E_{P/Q}{}^{0'}) \quad ...(I)$$

$$Q_{ads} + 2Mo(VI)_{sol} \xrightarrow{k_{cat}} P_{ads} + (Mo(V)_2)_{sol} \quad ...(II)$$

where reaction between Q_{ads} and $Mo(VI)_{sol}$ is the rds. The $E_{P/Q}{}^{0'}$ is the formal potential of the surface confined redox species (P/Q). It is –0.08 V (Fig.5 curve(b)). The number of electrons in rxn. (I) is found to be 2 from the wave shape analyses of C3/A3 of MGCE and the details of the monolayer analyses will be published elsewhere[36].

The surface redox catalysis at C3/A3 is examined by analysing the CV data of C3/A3 at bare GCE in Mo(VI) containing acid solution using the method, developed by Andrieux and Saveant[35]. The catalytic rate constant, k_{cat}, is estimated, as done in previous studies[37,38] by using the experimental dimensionless peak current function values $[i_{pC3} / \{nFAc_{Mo(VI)} / D_{Mo(VI)}{}^{1/2} (nFv/RT)^{1/2}\}]$ and the Fig.1 given in ref. [35] in which the dimensionless peak current function is given as a function of

$$\log\left[\frac{lk_{cat}\,\tau_t}{D_{MoVI)^{1/2}}}\left(\frac{nFv}{RT}\right)^{1/2}\right] \quad ...(9)$$

The average k_{cat} value calculated (with l=1, since monolayer) at various Mo(VI) concentrations in the range 1.5 to 7.0 mM (τ_t = 0.6- 2.1 x 10^{-10} mol cm^{-2}), using the literature value $D_{Mo(VI)}$ = 0.54x10^{-5} $cm^{-2}s^{-1}$ in 0.1 M H_2SO_4 [2], is found to be (0.60±0.15) x$10^3M^{-1}s^{-1}$.

Processes at C4/A4 and C5/A5

As shown in Fig. 7, the predominant peaks C4 and C5 are accompanied by the reverse anodic peaks A4 and A5 only at high scan rates, as observed with C3/A3 peak. However, the i-t curve of CPE at –500 mV (after C5) in Mo(VI) solution, Fig. 6, shows an initial current rise and then starts decreasing to the base current value after the completion of electrolysis as normally observed for any uncomplicated system. The integrated charge, corrected for the background processes, in this case indicates the consumption of one Faraday equivalent per mole of Mo(VI) (1.07±0.18 Faraday, over four independent measurements). Thus the absence of A4 and A5 at very slow scan rates, Fig. 7, may result from moderately rapid dimerisation reaction of the reduced molybdate to $Mo(V)_2$ as confirmed by UV spectra of the CPE product solution after C5 (Fig. 6B). The dimerisation of the fully reduced molybdate apparently requires a few thousand milliseconds under the conditions employed in Fig. 7.

Peak current, i_{pC4}, versus $c_{Mo(VI)}$ and $\log(i_{pC4})$–$\log(v)$ plots show that the processes at C4 (or C5) are under adsorption and diffusion-controlled. As shown in Fig. 8A, i_{pC4} varies with $c_{Mo(VI)}$ showing three

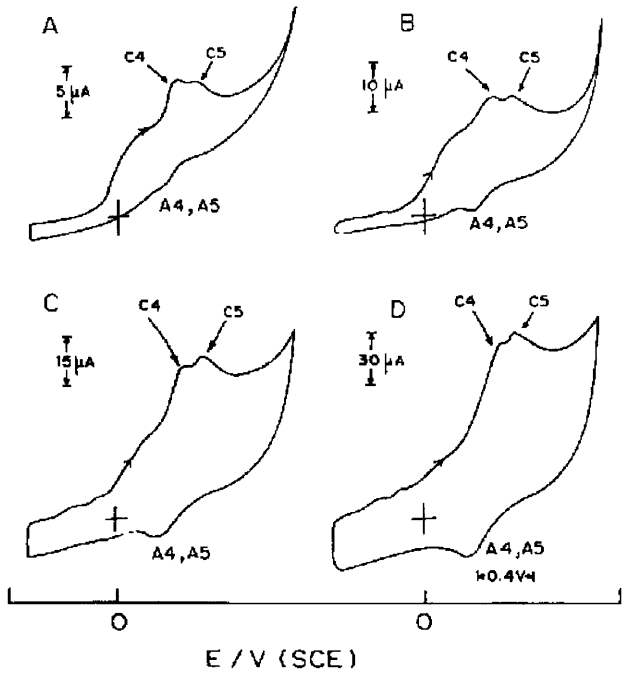

Fig. 7 Cyclic voltammograms of 12 mM Mo(VI) in 0.1 M H_2SO_4 at different scan rates (mVs^{-1}) : (A) 5; (B) 50; (C) 200; (D) 600.

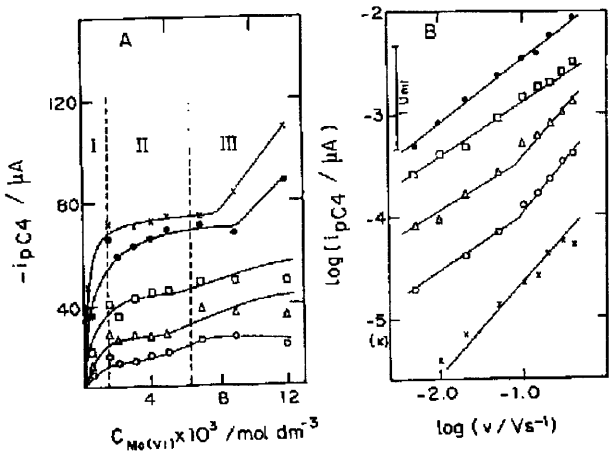

Fig. 8 (A) i_{pC4} vs $c_{Mo(VI)}$ in 0.1 M H_2SO_4 for C4 peak at different scan rates (mVs^{-1}): (o)50; (Δ) 100; (□) 200; (●) 400; (X) 600 (B) log (i_{pC4}) vs log (scan rate/Vs^{-1}) plots for different $c_{Mo(VI)}$ in 0.1 M H_2SO_4 : (X) 0.5; (o) 2; (Δ) 5; (□) 7; (●) 9 mM. (The Y axis is shifted in the upward direction by 0.4 units for increasing $c_{Mo(VI)}$)

characteristic zones. If now i_{pC4} for a particular concentration with different v are plotted, Fig. 8B is obtained. In zone I, the peak current is proportional to the scan rate with a slope 1.0 between log(i_{pC4}) and log(v), indicating that the surface electron transfer mainly contributes to the observed current. In zone II, slow interaction kinetics between adsorbed and soluble Mo(VI) is presumed to dominate[39]: a slope of 0.5 at slow scan rates (diffusion controlled electron transfer) and 1.0 at high scan rates (surface electron transfer) are observed. In zone III, log(i_{pC4}) against log(v) gives slope 0.5 in the entire scan rate region examined. A similar behaviour has been reported recently in the literature for cytochrome C on Hg[39].

The above characteristics can be seen more clearly in the variation of the current function ($i_p/cv^{1/2}$) with v at low and high Mo(VI) concentrations. This is presented in Fig. 9. When the bulk Mo(VI) concentration is quite high, the current function ratio remains constant at low v, further decreases with v and increases later only at very high scan rates. But with solutions of lower Mo(VI) concentrations the current function ratio increases steeply with v right from v =5 mVs^{-1}. This indicates predominant weak reactant adsorption at low concentrations. This behaviour is predicted when $c_{Mo(VI)} \exp(-\Delta G^0/RT)^{-1} \geq 2$, where ΔG^0 is the standard Gibbs free energy of adsorption isotherm[40,41].

The peaks C4 and C5 shift to more cathodic potentials and the peak potential separation (cathodic vs anodic) also increases when the experimental scan rate v is increased. The electrode kinetic parameter αn_a is evaluated for the C4 and C5 processes from E_{pc} vs log(v) plots. These plots are analysed at higher Mo(VI) concentrations and lower scan rates where adsorption must have a lesser relative influence on the voltammograms[28,40]. The average αn_a values for C4 and C5 are around 0.65 and 0.63 respectively for $c_{Mo(VI)}$ beyond 5 mM in the scan rate range 5-200 mVs^{-1}. If α is considered to be equal to 0.5, then n_a = 1 indicating that Mo(VI) diffusing from solution is reduced with one electron both at C4 and C5.

The formal specific rate constants (k_s) for the processes at C4 and C5 are calculated by the Nicholson's semiquantitative method using the equation $k_s = 11.083\ (D_{Mo(VI)}v)^{1/2}\psi$, where ψ is estimated corresponding to experimental ΔE_p from the working curve assuming that α = 0.5, $D_{Mo(VI)} = D_{Mo(V)}$, n = 1 and T = 298 K[42]. The average k_s values obtained for $c_{Mo(VI)}$ > 5 mM at v = 20 to 200 mVs^{-1} are (2.44± 0.62)x10^{-3} cm s^{-1} and (0.91± 0.34)x10^{-3} cm s^{-1} for C4 and C5 processes respectively. k_s for C4 is almost thrice larger than the value for C5.

Charge Transfer Mechanisms

The coulometric results of this study indicate that the peaks C1 to C5 together correspond to a one electron reduction. Further, the spectrum taken after

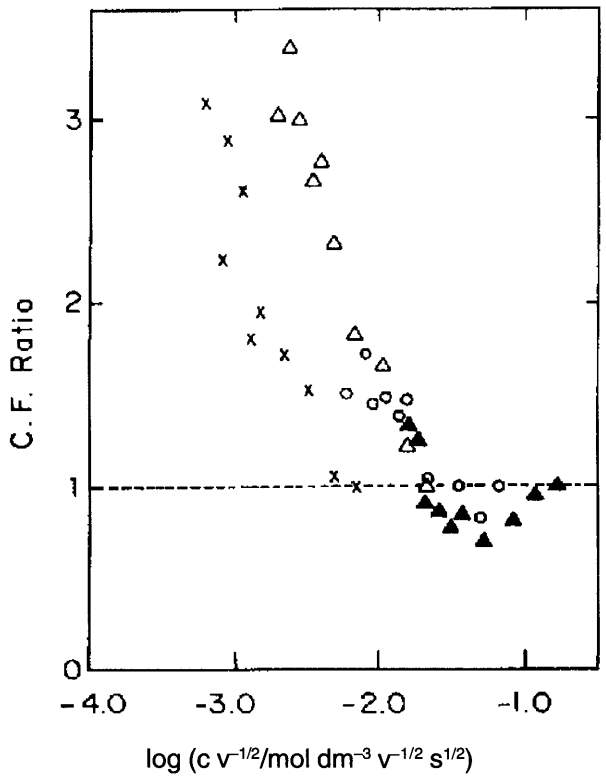

Fig. 9 Plots of ratio of current function ($i_{pC4}\, c_{Mo(VI)}^{-1}\, v^{-1/2}$) of peak C4 to the current function values as $c_{Mo(VI)}\, v^{-1/2} \rightarrow \infty$, taken as the $i_{pC4}\, c_{Mo(VI)}^{-1}\, v^{-1/2}$ value at the lowest v (5 mV s^{-1}), against $\log(c_{Mo(VI)}\, v^{-1/2})$: (**X**) 0.5; (Δ) 1.5; (**O**)5; (▲) 12 mM Mo(VI) in 0.1 M H_2SO_4.

completion of CPE after C5 peak corresponds to that of $Mo(V)_2$ (Fig.6B). It should be assumed from these data that the peaks C1 to C5 are due to the reduction of Mo(VI) to Mo(V). A similar situation, but with three polarographic waves, has been reported concerning Mo(VI) reduction on Hg electrode[8a].

The existence of five peaks corresponding to Mo(VI) to Mo(V) on GCE can be explained by a stepwise reduction of a single Mo(VI) species with conproportionation reaction following the charge transfer step or by respective reduction of five different forms of Mo(VI) species in solution.

The XPS identification of Mo(V) as the reduction product both at C1 peak and C2 peak (Fig.3), and the fact that these two peaks do not present any complications (as with C3 peak), clearly suggest that these two peaks do not correspond to stepwise reduction of single species. C1 and C2 can arise due to reduction of two forms of molybdate(VI) species, $Mo(VI)_A$ and $Mo(VI)_B$, which are in equilibrium in H_2SO_4 solution. The processes can be represented as

$$\text{At C1/A1: } (Mo(VI)_A)_{ads} + e \rightleftarrows Mo(V)_{ads} \quad ...(III)$$

$$\text{At C2/A2: } (Mo(VI)_B)_{ads} + e \rightleftarrows Mo(V)_{ads} \quad ...(IV)$$

The surface redox catalytic behaviour of C3/A3 (Fig. 4), wherein the Mo(VI) in solution is involved in generating the C3 reactant in the surface layer (Fig. 5), can be easily understood if the reduction products of C1 and C2 take part in the electron transfer step at C3 as follows.

At C3/A3:

$$(Mo(V))_{ads} + 2e \rightleftarrows Mo(III))_{ads} \quad ...(V)$$

$$Mo(III))_{ads} + 2Mo(VI)_{sol} \xrightarrow{k_{cat}} Mo(V)_{ads} + (Mo(V)_2)_{sol} \quad ...(VI)$$

The solution product, namely $(Mo(V)_2)$, is consistent with the UV spectral identification of CPE product solution at C3 peak (Fig. 6B).

Detailed analyses of individual processes have shown that the cathodic peaks C1 and C2 originate from surface bound species (Fig. 2), and adsorption effects are involved in the reduction mechanisms for peaks C4 and C5 (Fig. 9). Since adsorption leads to the possibility of splitting of a reduction wave to a single kind of electroactive species[40], the adsorption peaks C1 and C2 and diffusion controlled quasireversible peaks C4 and C5 can be related. The relative heights (ρ) of adsorption peak and diffusion peak provide a more detailed proof of this interpretation. ρ of peaks C1 and C4 change with v, as one expects for assignment to surface and diffusion waves respectively[40]. This is shown in Fig. 10. It is clear that ρ is a linear function of $v^{1/2}c^{-1}_{Mo(VI)}$ at slower scan rates. The negative deviation at high $v^{1/2}$ in this case is a strong evidence for a weaker adsorption of reactant in the C4 region[40,41]. Note that the extent of deviation is more with 0.5 mM (Fig. 10A) indicating remarkable weak reactant adsorption compared to 7 and 9 mM (Fig.10B), in agreement with the conclusions already drawn in Fig. 9. Behaviour similar to Fig. 10 is observed when the peak current ratio of C2 and C5 is plotted against $v^{1/2}c^{-1}_{Mo(VI)}$. So it is reasonable to suggest that C1 is the prepeak of C4, and C2 is the prepeak of C5. As $Mo(VI)_A$ and $Mo(VI)_B$ in adsorbed state undergo reduction at C1 and C2, their dissolved forms can be postulated to take part in the reaction at C4 and C5.

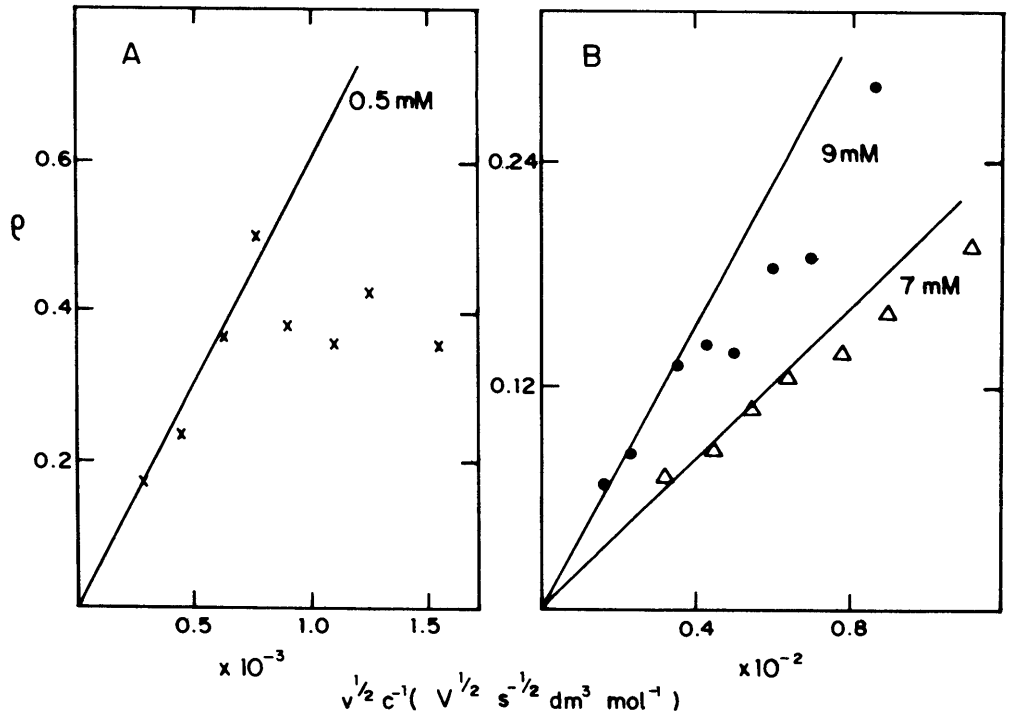

Fig. 10 Plots of ratio (ρ) of the peak currents of C1 and C4 against $v^{1/2} c_{Mo(VI)}^{-1}$ at different $c_{Mo(VI)}$ in 0.1 M H_2SO_4: (A) 0.5 mM (B) (Δ) 7 mM, (●) 9 mM

With $\alpha n_a = 0.65$ for the charge transfer step of $(Mo(VI)_A)_{sol}$ reduction at C4, in conjunction with the UV identification of $(Mo(V)_2)_{sol}$ as the corresponding reduction product (Fig.6B), it is possible to hypothesise the mechanism of $(Mo(VI)_A)_{sol}$ reduction, if we assume that the rds is the first step of the mechanism and it should be one electron step[43]. Under these conditions the reduction can proceed according to either of the following mechanisms:

At C4:

Scheme A

$$2\ \{\ (Mo(VI)_A)_{sol} + e \rightarrow Mo(V)_{sol}\ \}\ (rds) \quad ...(VII)$$

$$2Mo(V)_{sol} \rightleftarrows (Mo(V)_2)_{sol} \quad ...(VIII)$$

$$2(Mo(VI)_A)_{sol} + 2e \rightarrow (Mo(V)_2)_{sol} \quad ...(IX)$$

Scheme B

$$(Mo(VI)_A)_{sol} + e \rightarrow Mo(V)_{sol}\ (rds) \quad ...(X)$$

$$(Mo(VI)_A)_{sol} + Mo(V)_{sol} + e \rightleftarrows (Mo(V)_2)_{sol} \quad ...(XI)$$

$$2(Mo(VI)_A)_{sol} + 2e \rightarrow (Mo(V)_2)_{sol} \quad ...(IX)$$

Both the mechanisms require that the total number of electrons exchanged in the overall heterogeneous process is two; but the stoichiometric number (number of times rds occurs) is two for the former and one for the latter mechanism.

The additional reaction at C4 due to the weak adsorption of the reactant $(Mo(VI)_A)$ is as follows.

$$2(Mo(VI)_A)_{ads} + 2e \rightarrow (Mo(V)_2)_{sol} \quad ...(XII)$$

For the reduction at C5, the same reasoning can be applied to the reduction of $Mo(VI)_B$ species. Thus at C5 $(Mo(VI)_B)_{sol}$ can get reduced following the mechanism similar to reactions (VII) to (XI); and $(Mo(VI)_B)_{ads}$ following rxn. (XII).

There is a major change in the Mo(VI) cyclic voltammogram for which the cathodic cycle is reversed at –200 mV compared to that with cathodic switching potential –1000 mV (Fig.1). The voltammogram obtained between +500 and –200 mV, where the more negative peaks C4, C5, A4 and A5 are still absent, the first three anodic peaks A1, A2 and A3 appear in the reverse sweep (Fig. 1 curve (b)). On the other hand, when sweeping window is extended to –1000 mV which is sufficient to include C4, C5, A4 and A5, the peaks A1, A2 and A3 completely disappear (Fig. 1 curve (a)). The disappearance of A1, A2 and A3 in the latter case must be related to the desorption of the C3 product at more negative potential and its oxidation at A4 and A5 to an electroinactive Mo(VI) form which is strongly

adsorbed on GCE surface until the potential is increased beyond E_{sur}^{0}, of C1/A1. The substantial increase in the anodic part of GCE background current (curve (a) vs curve (c) in Fig. 1) supports this hypothesis.

Two forms of Mo(VI) species are considered to explain the five reduction peaks C1,C2, C3, C4, and C5 in the Mo(VI) reduction to Mo(V) on GCE. In H_2SO_4 acid solutions in the concentration range 1M to 0.01 M, molybdate(VI) is known to exist as monomers ($Mo(OH)_5O^-$ [12], $Mo(OH)_6$ and $Mo(OH)_5(H_2O)^+$ [14], $Mo(OH)_4SO_4^{2-}$ [15]) and dimers ($Mo_2O(OH)_8(H_2O)^{2+}$ and $Mo_2O(OH)_7(H_2O)_2^{3+}$ [14]), with the monomeric anionic species ca. $Mo(OH)_5O^-$ and neutral species ca. $Mo(OH)_6$ as predominant in H_2SO_4 acids in the range 0.2 M to 0.01 M[14]. Thus, at 0.1 M H_2SO_4 used in the present studies these two are the likely electroactive species with $Mo(OH)_5O^-$ for C1 (and C4) peak with repulsive interaction, and $Mo(OH)_6$ for C2 (and C5) peak with attractive interaction. Further work on Mo(VI) specification in H_2SO_4 solutions is in progress to identify the exact form of the two electroactive Mo(VI) species associated with respective CV peaks.

Conclusions

Our results and their analysis show that the complexity with which Mo(VI) ion gets reduced to Mo(V) on GCE in 0.1 M H_2SO_4 (via five reduction peaks) is due to two forms of Mo(VI) species undergoing reduction. The further complexity arises because the electron transfer process of each of the Mo(VI) species occurs by three reduction mechanisms: (i) diffusion controlled quasireversible reduction of dissolved species (C4 or C5); (ii) reversible reduction due to strong product adsorption (C1 or C2); and (iii) reduction due to weak reactant adsorption (at C4 or C5).

Further to this, at the potential of C3 peak, lying in between the surface prepeaks C1 and C2 and solution peaks C4 and C5, the product of C1 and C2, viz., the surface immobilised Mo(V) undergoes two-electron reduction to another surface bound component Mo(III). In addition, the product of C3 ($Mo(III)_{ads}$) is encountered with the solution phase Mo(VI) in a conproportionation reaction resulting in the catalytic regeneration of $Mo(V)_{ads}$ under suitable experimental conditions (low v and high Mo(VI) concentrations).

Acknowledgement

The authors are grateful to the Council of Scientific and Industrial Research, New Delhi for awarding Fellowship to one of the authors (G I).

References

1 T E Edmonds *Anal Chim Acta* **116** (1980) 323

2 I M Kolthoff and I Hodara *J Electroanal Chem* **4** (1962) 369

3 J J Wittick and G A Rechnitz *Anal Chem* **37** (1965) 816

4 M N Hull *J Electroanal Chem* **51** (1974) 57

5 P Chalipoyil and F C Anson *Inorg Chem* **17** (1978) 2518

6 M I Paffet and F C Anson *Inorg Chem* **20** (1981) 3967

7 (a) S Himeno and A Saito *J Electroanal Chem* **130** (1981) 263; (b) *ibid* **152** (1983) 163

8 (a) K Yokoi, T Ozeki, I Watanabe and S Ikeda *J Electroanal. Chem* **132** (1982) 191; (b) *ibid* **133** (1982) 73

9 K Yokoi, N Ogawa, I Watanabe and S Ikeda *J Electroanal Chem* **153** (1983) 235

10 K Yokoi, I Watanabe and S Ikeda *J Electroanal Chem* **217** (1987) 305

11 M Berotti and R Tokoro *J Electroanal Chem* **360** (1993) 39

12 K-H Tytko and O Glemser *Adv Inorg Chem Radiochem* **19** (1976) 239

13 M T Pope *Heteropoly and Homopoly Oxometallates* Springer Verlag Berlin (1983)

14 (a) J J Cruywagen, J B B Heyns and E F C H Rohwer *J Inorg Nucl Chem* **38** (1976) 2033; (b) *ibid* **40** (1978) 53; (c) J J Cruywagen, (Sep. 1994) (personal comm.)

15 S Himeno, Y Ueda and M Hasegawa *Inorg Chim Acta* **73** (1982) 255

16 I G Shafran, V P Rozenblyum and G A Shteimberg *Tr Vses Nauch-Issled Inst Kim Veshchestv* **31** (1969) 171 (see ref. [18])

17 V F Toropova, V A Vekslina and N G Chovnik *Zh Analit Kim* **28** (1973) 967 (CA:79;73203)

18 P Zanello, G Raspi and Cinquantini *Talanta* **24** (1977) 25

19 S I Saradyan, P K Agasyan and E R Ncklaeva *Arm Khim Zh* **38** (1973) 281 (CA:104;26128p)

20 K Chandrasekara Pillai and G Ilangovan *Bull Electrochem* **9** (1993) 392

21 G Ilangovan and K Chandrasekara Pillai *Langmuir* **13** (1997) 566

22 G Ilangovan and K Chandrasekara Pillai *J Electroanal Chem* **431** (1997) 11

23 G Ilangovan and K Chandrasekara Pillai *J Solid State Electrochem* **3** (1999) 357

24 G Ilangovan and K Chandrasekara Pillai *J Solid State Electrochem* **3** (1999) 474

25 A P Brown and F C Anson *Anal Chem* **49** (1977) 1589

26 D F Smith, K Willman, K Kuo and R W Murray *J Electroanal Chem* **95** (1979) 217

27 J Facci and R W Murray *Anal Chem* **54** (1982) 772

28 E Laviron *J Electroanal Chem* **52** (1974) 355
29 W Grunert, A Y Stakheev, R Feldhaus, K Anders, E S Sphire and K M Mnachev *J Phy Chem* **95** (1991) 1323
30 C R Clayton and Y C Lu *Sur Interf Anal* **14** (1989) 66
31 R Rodriguez-Amaro, M Sanches, E Munoz, J J Ruiz and L Camacho *J Electrochem Soc* **143** (1996) 2132
32 K Kano and B Uno *Anal Chem* **65** (1993) 1088
33 W H Press, B P Flanaery, S A Tenkolsky and W T Wetterling *Numerical Receipes* Cambridge University Press (1988)
34 A J Bard and K S V Santhanam *Electroanalytical Chemistry* (Ed. A J Bard) Dekker NY **4** (1970) 215
35 C P Andrieux and J M Saveant *J Electroanal Chem* **93** (1978) 163
36 G Ilangovan and K Chandrasekara Pillai (under submission)
37 H Jaegfeldt, T Kuwana and G Johansson *J Am Chem Soc* **105** (1983) 1805
38 H Jaegfeldt, A Tortensson, L Gorton and G Johannson *Anal Chem* **53** (1979) 1981
39 D Zhang, G S Wilson and K Niki *Anal Chem* **66** (1994) 3873
40 R W Wopschall and I Shain *Anal Chem* **39** (1967) 1514
41 J F Rusling and M Y Brooks *J Electroanal Chem* **163** (1984) 277
42 A J Bard and L R Faulkner *Electrochemical Methods* John Wiley Sons NY (1980)
43 J O'M Bockris and A K N Reddy *Modern Electrochemistry* Plenum NY **2** (1990)